CRM^R

CENTRE DE RECERCA MATEMÀTICA

A time dependent model to determine the thermal conductivity of a nanofluid

T.G. Myers, M.M. MacDevette, H. Ribera

A TIME DEPENDENT MODEL TO DETERMINE THE THERMAL CONDUCTIVITY OF A NANOFLUID

T.G. MYERS, M.M. MACDEVETTE AND H. RIBERA

ABSTRACT. In this paper we analyse the time-dependent heat equations over a finite domain to determine expressions for the thermal diffusivity and conductivity of a nanofluid (where a nanofluid is a fluid containing nanoparticles with average size below 100nm). Due to the complexity of the standard mathematical analysis of this problem we employ a well-known approximate solution technique known as the Heat Balance Integral Method. This allows us to derive simple analytical expressions for the thermal properties, which appear to depend primarily on the volume fraction and liquid properties. The model is shown to compare well with experimental data taken from the literature even up to relatively high concentrations and predicts significantly higher values than the Maxwell model for volume fractions approximately greater than 1%. The results suggest that the difficulty in reproducing the high values of conductivity observed experimentally may stem from the use of a static heat flow model applied over an infinite domain rather than applying a dynamic model over a finite domain.

1. INTRODUCTION

There exists a vast literature on the enhanced thermal properties of nanofluids when compared to their base fluids. The often remarkable enhancement then suggests nanofluids as the solution for heat removal in many modern electronic devices. However there are discrepancies and much debate over experimental findings and so far no satisfactory mathematical model has been proposed to describe the thermal response of a nanofluid (Buongiorno *et al.*, 2009; Eastman *et al.*, 2004; Eastman *et al.*, 2001; Koo & Kleinstreuer, 2004; Prasher *et al.*, 2005).

The classical analysis of heat conduction for solid-in-liquid suspensions is that of Maxwell (Maxwell, 1891), based on effective medium theory. Das *et al.* (Das *et al.*, 2008) describe in detail how this result is derived. The nanofluid is assumed to occupy a sphere of radius r_0. This sphere is approximated as a homogeneous medium containing an 'effective fluid' and the steady state heat equation is solved *in the region outside of the sphere, $r \in [r_0, \infty]$*, subject to continuity of temperature and heat flux at the boundary $r = r_0$. The result obtained from this analysis is then applied to describe the thermal response of an infinite volume of liquid surrounding a single particle. Using the principle of superposition this

last result may then be used to approximate the temperature profile for a fluid containing many particles. The two temperature expressions (outside the sphere of radius r_0 and that obtained by superposition) are finally equated to determine an appropriate thermal conductivity for the effective fluid:

$$(1) \qquad k_e = \left[\frac{2k_l + k_p + 2\phi(k_p - k_l)}{2k_l + k_p - \phi(k_p - k_l)} \right] k_l \,,$$

where k_e, k_p, k_l represent the effective, particle and liquid thermal conductivity respectively and ϕ is the particle volume fraction.

There are obvious problems with the Maxwell model. Firstly, it is based on analysing the heat flow in the material surrounding an equivalent nanofluid and the heat flow around a particle, as opposed to analysing the actual nanofluid or particle behaviour. The analysis is carried out over an infinite region. The principle of superposition is then applied to determine the response around infinitely many particles, each separated by an infinite volume of fluid. Hence the result can only be applied to a highly disperse fluid where the particles are so far apart that an energy change in one has a negligible effect on any other particle. This approach will clearly lead to problems as the particle concentration increases. Further, the Maxwell model is based on a steady-state solution but in general one would wish to analyse how a nanofluid responds in a time-dependent situation.

Despite the various drawbacks the Maxwell model is known to work well with low volume fraction fluids containing relatively large particles (microscale or above). Only when the particle size decreases to the nanoscale do problems become apparent. For example, for sufficiently small volume fractions, ϕ, the relation between the conductivity and volume fraction may be linearised

$$(2) \qquad \frac{k_e}{k_l} \approx 1 + C_k \phi \,,$$

where C_k is known as the conductive enhancement coefficient. Keblinski et al (Keblinski et $al.$, 2005) compared the data from various groups working with nanofluids and found that for most of the data $C_k \approx 5$ whilst the Maxwell model predicts $C_k \approx 3$. A linear approximation to the Maxwell model follows easily from (1) by first noting k_p is much larger than k_l (see Table 1) and so k_l may be neglected in the square brackets. Then, using a binomial expansion based on small ϕ we obtain the correct enhancement coefficient,

$$(3) \qquad k_e \approx \left[\frac{k_p + 2\phi k_p}{k_p - \phi k_p} \right] k_l \approx (1 + 2\phi)(1 + \phi)k_l \approx (1 + 3\phi)k_l \,,$$

which coincides with the conclusions of Keblinski et $al.$ (Keblinski et $al.$, 2005).

In an attempt to improve the fit between theory and experiment various researchers have extended or modified Maxwell's model. The Hamilton and Crosser (Hamilton & Crosser, 1962) model is a slight adaptation to account for particle shape: for spherical particles it reproduces the Maxwell result. Yu and Choi

(Yu & Choi, 2003) reapply the Maxwell result to include the effect of a nanolayer on the particle surface, they subsequently extend this to the Hamilton-Crosser model (Yu & Choi, 2004). However, the thermal conductivity and thickness of this nanolayer are unknown. Wood and Ashcroft (Wood & Ashcroft, 1977) propose a multi-component version of the Maxwell model which is then extended by Wang *et al.* (Wang *et al.*, 2003) to incorporate particle clustering for non-metallic particles and is valid for very low volume fractions (below 0.5%). In each case the introduction of new effects and new parameters permits better agreement with certain experiments. For example, in (Yu & Choi, 2003) choosing a nanolayer with thickness 2nm and nanolayer conductivity greater than ten times that of the base fluid leads to excellent agreement with data for a CuO-Ethylene glycol suspension. In (Das *et al.*, 2008) a comprehensive list of variations to Maxwell's model and similar theories are described. They go on to describe a number of dynamic models which incorporate effects such as Brownian motion and nanoconvection. Examples of these include the work of Koo and Kleinstreuer (Koo & Kleinstreuer, 2004) who alter the Maxwell model by adding on a term to account for Brownian motion. Prasher *et al.* (Prasher *et al.*, 2005) multiply the Maxwell result to include a Brownian factor. Their model has two free parameters which are then chosen to match experiment.

Tillman and Hill (Tillman & Hill, 2007) take a slightly different approach by focussing on the effect of the nanolayer. They analyse the steady-state heat equation by first assuming some asymmetry which motivates a solution involving Legendre polynomials (the functions that describe the polar angle variation of the solution). Their nanolayer has a varying conductivity and unknown thickness and they investigate possible forms for $k_{layer}(r)$. They found the nanolayer thickness as a percentage of the particle radius, ranging between 19% to 22%, when k_{layer} is a polynomial of degree greater than 23.

The motivation behind the above studies and a host of others including, for example, particle aggregation or based on matching experimental observation, is the lack of a theory which matches a wide range of experimental data. The Maxwell model indicates thermal conductivity varies solely with volume fraction, however, there is evidence indicating variation due to size, shape, particle material, additives, pH and temperature effects (Philip & Shima, 2012) (and often evidence to the contrary (Philip & Shima, 2012)). Brownian motion has been shown to provide improved agreement with certain data yet Keblinski *et al* (Keblinski *et al.*, 2002) show that the time-scale for Brownian motion is so much slower than thermal diffusion that it is unlikely to play an important role in heat transfer. Of course, since Maxwell is steady-state any modification of Maxwell (or models derived from it) would not be able to take into account different time-scales. Liquid layers have been inferred via experiments and simulation, but only around 1nm thick, which then cannot account for a sufficient increase in conductivity (Eastman *et al.*, 2004). Keblinski *et al.* (Keblinski *et al.*, 2008) suggest that much of the controversy over thermal conductance prediction may be due

to the assumption of well dispersed particles, when in fact particle aggregation may take place.

Motivated by the obvious drawbacks of the Maxwell model and the difficulties in matching experimental evidence and recent advances in the understanding of nano phenomena in this paper we take a different theoretical approach. Our mathematical model, described in §3 will involve the time-dependent response of a system containing a single nanoparticle surrounded by a finite volume of fluid (so fitting into the dynamic category of models described in (Das *et al.*, 2008)). This will be matched to the response of an equivalent fluid volume with an unknown diffusivity. Given the mathematical complexity of this approach, in §2 we will first describe an accurate approximate mathematical method for solving the heat equation over a finite domain. In §4 we compare the expression for the thermal conductivity determined through the present analysis with that of Maxwell and experimental data. This shows that the present model not only predicts a significantly larger enhancement than Maxwell, but also matches well to a large range of data, without the need for additions such as a nanolayer or Brownian motion. Further, since the analysis is carried out over a finite volume it is not restricted to highly disperse fluids.

2. The Heat Balance Integral Method

The mathematical model laid out in §3 will require the solution of time-dependent heat equations in two adjacent finite volumes. The exact mathematical solution is cumbersome, involving infinite series, and so it is difficult to isolate the dependence on physical parameters. For this reason we will employ an approximate solution technique known as the Heat Balance Integral Method (HBIM). In the following we will illustrate the HBIM through an example, which will then be used in our subsequent analysis. In §3.1 we will determine the exact solution for the simpler problem of heat flow in a single fluid volume, this will then be compared to the HBIM to solution to verify its accuracy.

Consider the standard thermal problem, defined on a semi-infinite domain, where a material initially at a constant temperature is heated to a different temperature at the boundary $y = 0$. In non-dimensional form this may be written

$$(4) \qquad \frac{\partial u}{\partial t} = \frac{\partial^2 u}{\partial y^2} \qquad u(0,t) = 1 \qquad u|_{y \to \infty} \to 0 \qquad u(y,0) = 0 \ .$$

The HBIM involves choosing a simple function to approximate the temperature over a finite region $\delta(t)$, known as the heat penetration depth. Since the heat equation has infinite speed of propagation the heat penetration depth is a notional concept. For $y \geq \delta$ the temperature change above the initial value is negligible (although we do not define what constitutes negligible). For this example the heat penetration depth would be defined by the boundary conditions $u(\delta, t) = 0$ and $u_y(\delta, t) = 0$.

If the approximating function is a polynomial of the form

(5)
$$u = a_0 + a_1 \left(1 - \frac{y}{\delta}\right) + a_n \left(1 - \frac{y}{\delta}\right)^n ,$$

then the conditions $u(\delta, t) = 0$ and $u_y(\delta, t) = 0$ determine $a_0 = a_1 = 0$, the condition at $y = 0$ determines $a_n = 1$ and so

(6)
$$u = \left(1 - \frac{y}{\delta}\right)^n .$$

The expression for u involves two unknowns, $\delta(t)$ and n. The heat penetration depth is determined by integrating the heat equation over the region $y \in [0, \delta]$

(7)
$$\int_0^\delta \frac{\partial u}{\partial t} \, dy = \int_0^\delta \frac{\partial^2 u}{\partial y^2} \, dy .$$

This is termed the heat balance integral. Since $u(\delta, t) = u_y(\delta, t) = 0$ this leads to

(8)
$$\frac{d}{dt} \int_0^\delta u \, dy = -\left. \frac{\partial u}{\partial y} \right|_{y=0} .$$

Substituting for u from equation (6) leads to a single ordinary differential equation for δ with solution

(9)
$$\delta = \sqrt{2n(n+1)t} ,$$

where $\delta(0) = 0$.

The standard HBIM takes $n = 2$, although there are many other possibilities, often chosen through knowledge of an exact solution, see (Mitchell & Myers, 2010). Myers (Myers, 2009) developed a method, which minimises the least-squares error when the approximate function is substituted back into the heat equation. This not only ensures a globally accurate representation but also removes the need for an exact solution. With the above problem the value of n that minimises the error is $n = 2.233$: this value leads to excellent agreement with the exact solution.

For problems over a finite domain the HBIM generally involves two stages. The first is as described above, this lasts until the heat penetrates to the boundary. In the second stage the boundary temperature, rather than δ, is the second unknown. A more detailed explanation of the HBIM, error minimisation and further examples are provided in (Mitchell & Myers, 2010; Mitchell & Myers, 2010; Myers, 2009; Myers, 2010).

3. Thermal analysis of a particle-fluid system

To describe the thermal response of a nanoparticle in a fluid consider a spherical volume of fluid, with radius R, containing a solid particle, with radius r_p. The

radius R is related to the volume fraction in the following manner. For a given volume V, the volume fraction of particles is

$$(10) \qquad \phi = \frac{(4/3)\pi r_p^3 N}{V}$$

where N is the number of particles contained in V. If we divide the volume into N equal components of radius R then each volume $V = (4/3)\pi R^3$ contains a single nanoparticle and so

$$(11) \qquad \phi = \frac{(4/3)\pi r_p^3}{(4/3)\pi R^3} = \frac{r_p^3}{R^3} \,.$$

A disperse fluid, with few particles, will have R large and hence $r_p/R \ll 1$, whilst a higher concentration of particles will result in higher r_p/R. For a known volume V containing N particles we may define $R = \sqrt[3]{3V/(4\pi N)}$.

The heat equations in the particle and liquid are

$$(12) \qquad \frac{\partial T}{\partial t} = \frac{\alpha_p}{r^2}\frac{\partial}{\partial r}\left(r^2\frac{\partial T}{\partial r}\right) \qquad r \in [0, r_p]$$

$$(13) \qquad \frac{\partial \theta}{\partial t} = \frac{\alpha_l}{r^2}\frac{\partial}{\partial r}\left(r^2\frac{\partial \theta}{\partial r}\right) \qquad r \in [r_p, R]\,.$$

Initially the fluid and particle have the same, constant temperature T_0. At time $t = 0$ the boundary $r = R$ is heated to a different temperature T_R. Assuming continuity of temperature and heat flux at the interface, the governing equations are then subject to the following boundary conditions

$$(14) \qquad \theta(r,0) = T(r,0) = T_0 \qquad \theta(R,t) = T_R \qquad \theta(r_p,t) = T(r_p,t) = T_p(t)$$

$$(15) \qquad k_l\left.\frac{\partial \theta}{\partial r}\right|_{r=r_p} = k_p\left.\frac{\partial T}{\partial r}\right|_{r=r_p} \qquad \left.\frac{\partial T}{\partial r}\right|_{r=0} = 0\,,$$

where T_p is the unknown temperature at the particle-fluid interface.

To simplify the problem we first write it in non-dimensional form

$$(16) \qquad \hat{T} = \frac{T - T_0}{T_R - T_0} \qquad \hat{r} = \frac{r}{R} \qquad \hat{t} = \frac{t}{\tau}\,,$$

and immediately drop the hat notation. Since the liquid occupies most of the volume we choose the standard diffusion time-scale $\tau = R^2/\alpha_l$ and then

$$(17) \qquad \frac{\partial T}{\partial t} = \frac{\alpha}{r^2}\frac{\partial}{\partial r}\left(r^2\frac{\partial T}{\partial r}\right) \qquad r \in [0, r_p]$$

$$(18) \qquad \frac{\partial \theta}{\partial t} = \frac{1}{r^2}\frac{\partial}{\partial r}\left(r^2\frac{\partial \theta}{\partial r}\right) \qquad r \in [r_p, 1]\,,$$

where $\alpha = \alpha_p/\alpha_l$ and r_p is now the original particle radius divided by R. The boundary conditions become

$$(19) \qquad \theta(r,0) = T(r,0) = 0 \qquad \theta(1,t) = 1 \qquad \theta(r_p,t) = T(r_p,t) = T_p(t)$$

$$(20) \qquad \left.\frac{\partial \theta}{\partial r}\right|_{r=r_p} = k \left.\frac{\partial T}{\partial r}\right|_{r=r_p} \qquad \left.\frac{\partial T}{\partial r}\right|_{r=0} = 0\,,$$

where $k = k_p/k_l$.

Table 1 contains a short list of thermal parameter values for typical substances used to make nanofluids. The values $\alpha = \alpha_p/\alpha_l \in [60, 1200]$ and $k = k_p/k_l \in [50, 1500]$ which appear in equations (17, 20) are both large. Therefore we may divide both sides of the appropriate equations by these values and find that the thermal problem in the particle may be well approximated by

$$(21) \qquad 0 \approx \frac{1}{r^2}\frac{\partial}{\partial r}\left(r^2\frac{\partial T}{\partial r}\right)$$

$$(22) \qquad T(r,0) = 0 \qquad T(r_p,t) = T_p(t) \qquad \left.\frac{\partial T}{\partial r}\right|_{r=r_p} \approx 0 \qquad \left.\frac{\partial T}{\partial r}\right|_{r=0} = 0\,.$$

For Al_2O_3 in water the largest error in this approximation comes through setting $T_r(r_p,t) \approx 0$, this error is of the order $k_l/k_p \approx 1/50 = 0.02$ or 2%. For Cu in ethylene glycol the largest error comes through the heat equation by neglecting the T_t term, which leads to errors of the order $\alpha_l/\alpha_p \approx 0.0008$ or 0.08%. The solution of this reduced system is simply

$$(23) \qquad T(r,t) = T_p(t)\,,$$

where $T_p(t)$ is an unknown function, however, the initial condition on T indicates $T_p(0) = 0$. This solution shows that the temperature is approximately independent of r in the nanoparticle. The physical interpretation of this is that changes in the liquid temperature are relatively slow: the speed of heat flow in the liquid is characterised by α_l/R^2 and α_l is much smaller than α_p. When a change in liquid temperature reaches the particle, which has a much higher diffusivity, it very rapidly distributes the heat. Consequently, on the liquid time-scale the particle temperature is approximately (to within the errors quoted above) the temperature at the liquid-particle boundary. Note, this result matches the experimental observations of Philip and Shima (Philip & Shima, 2012) that the conductivity of the solid does not dictate the conductivity of the nanofluid. It is also clear from simple equations, such as the Maxwell equation (1), as shown by the approximation (3), with an error of order k_l/k_p which is below 2% for the values quoted in Table 1.

The HBIM is well-known to be less accurate in spherical than Cartesian coordinates, particularly if the origin is included in the domain. In the following

Substance	Density ρ (kg/m^3)	Specific heat c (J/kg K)	Diffusivity α (m^2/s)	Conductivity k (W/m K)
Al$_2$0$_3$	4000	880	8.522×10^{-6}	30
Copper	8920	390	1.152×10^{-4}	401
Water	998	4190	1.387×10^{-7}	0.58
Ethylene Glycol	1110	2470	9.4102×10^{-8}	0.258

TABLE 1. Typical thermal parameter values for two nanoparticles and base fluids.

analysis we will work over the range $r \in [r_p, 1]$. For very low volume fractions, $r_p \to 0$, we will see that the results do not compare well with experimental data but for $\phi > 1\%$ the agreement is good. To improve the HBIM accuracy and to exploit the method described in the previous section we now transform the problem in the liquid to a Cartesian system, with heat applied at the left hand boundary, by making the change of variables

$$(24) \qquad \theta = \frac{u}{r} \qquad y = \frac{1-r}{1-r_p}.$$

The heat equation in the liquid is now

$$(25) \qquad \frac{\partial u}{\partial t} = \lambda \frac{\partial^2 u}{\partial y^2}$$

where $\lambda = 1/(1 - r_p)^2$ and is subject to

$$(26) \qquad u(y,0) = 0 \quad u(0,t) = 1 \quad u(1,t) = r_p T_p(t) \quad \left. \frac{\partial u}{\partial y} \right|_{y=1} = -(1 - r_p)T_p \,.$$

The domain $r \in [r_p, 1]$ is transformed to $y \in [0, 1]$ with the heat applied at $y = 0$. The HBIM analysis of this system requires two stages. In the first stage heat is applied at the boundary and penetrates to a depth $\delta \leq 1$, so the boundary conditions at $y = 1$ are replaced with

$$(27) \qquad u(\delta, t) = 0 \qquad \left. \frac{\partial u}{\partial y} \right|_{y=\delta} = 0 \,.$$

This is exactly the problem formulated in §2 (with time scaled by a factor λ) and so we define u by equation (6) with $n = 2.233$ and $\delta = \sqrt{2n(n+1)\lambda t}$. This stage ends when $\delta = 1$ at time $t = t_1 = 1/(2n(n+1)\lambda)$.

In the second stage the boundary conditions (26) apply and the HBIM analysis is slightly modified,

$$u = r_p T_p + (1 - r_p)T_p(1 - y) + (1 - T_p)(1 - y)^n \,. \tag{28}$$

In this case there is no δ, instead the boundary temperature, $T_p(t)$, is the unknown function of time. To allow continuity of temperature at $t = t_1$, $n = 2.233$ again (note the issues arising from switching n in different phases are discussed in (Mitchell & Myers, 2008)). The heat balance integral is applied over $y \in [0,1]$ and leads to

$$\frac{dT_p}{dt} = \Lambda(1 - T_p)\,, \tag{29}$$

where $\Lambda = n\lambda/c_T$ and $c_T = (1 + r_p)/2 - 1/(n + 1)$, hence

$$T_p = 1 - e^{-\Lambda(t - t_1)} \,. \tag{30}$$

The HBIM problem is now completely solved. In Stage 1 u is defined by (6), $\delta = \sqrt{2n(n + 1)\lambda t}$ and the particle temperature $T_p = 0$. This ends at time $t = t_1$. In Stage 2 u is defined by (28) and the particle temperature T_p by (30). The non-dimensional temperature in each stage is determined by the relation $\theta = u/r$.

3.1. **Equivalent fluid analysis.** To define an equivalent fluid we imagine a sphere of fluid with diffusivity α_e, in the non-dimensional system we write $\alpha' = \alpha_e/\alpha_l$. If the equivalent fluid temperature is denoted θ_e then the temperature is determined by

$$\frac{\partial \theta_e}{\partial t} = \frac{\alpha'}{r^2}\frac{\partial}{\partial r}\left(r^2\frac{\partial \theta}{\partial r}\right) \qquad \theta_e(1, t) = 1 \qquad \left.\frac{\partial \theta_e}{\partial r}\right|_{r=0} = 0 \,. \tag{31}$$

We define $u_e = r\theta_e$ and denote the temperature at $r = 0$ as $T_c(t)$. This is obviously the limit of the liquid thermal problem described in the previous section after setting $r_p = 0$ and writing T_c instead of T_p. Consequently we may use the previous solution.

In Stage 1 $T_c = 0$ and so the formulation matches the HBIM problem of §2 (with time scaled by the diffusivity α'). Hence the temperature in Stage 1 is described by equation (6) with $\delta' = \sqrt{2n(n + 1)\alpha't}$. This ends at time $t'_1 = 1/(2n(n+1)\alpha')$. In Stage 2 setting $r_p = 0$ and $T_p = T_c$ equation (28) gives

$$u_e = T_c(1 - y) + (1 - T_c)(1 - y)^n \tag{32}$$

where

$$T_c = 1 - e^{-\Lambda'(t - t'_1)} \tag{33}$$

and $\Lambda' = n\alpha'/c_{T0}$ and $c_{T0} = (n - 1)/(2(n + 1))$.

In fact, the thermal problem described by (31) has an exact solution obtained by separation of variables. This may be used to verify the HBIM solution. In the Cartesian system this is

$$(34) \qquad u_s = (1-y) + \sum_{n=1}^{N} 2\frac{(-1)^n}{\pi n} \sin(n\pi(1-y))e^{-n^2\pi^2\alpha' t},$$

where the subscript s denotes separable and $r = 1 - y$.

Equation (34) may be used to verify the HBIM solution given by equation (32). Since this system has no nanoparticle the equivalent fluid diffusivity is exactly the liquid value, $\alpha' = 1$. The two sets of solutions, with $\alpha' = 1$, are shown in Figure 1, the solid lines are the separable solutions and the dashed lines the HBIM solution at times $t = 0.02, 0.08, 0.2, 0.4$. The value of $t'_1 = 1/(2n(n+1)) = 0.069$ indicates that for $t = 0.02$ we must use the Stage 1 solution where u_e is given by equation (6) and $\delta' = 1/(0.04n(n+1))$ (recall δ' indicates the position where the HBIM method predicts the temperature rise is negligible). It may be observed that the separable solution is approximately zero just slightly beyond the end of the HBIM solution. For subsequent times the dashed curves are given by equation (32). In general it is clear that there is a good correspondence between the two sets of curves.
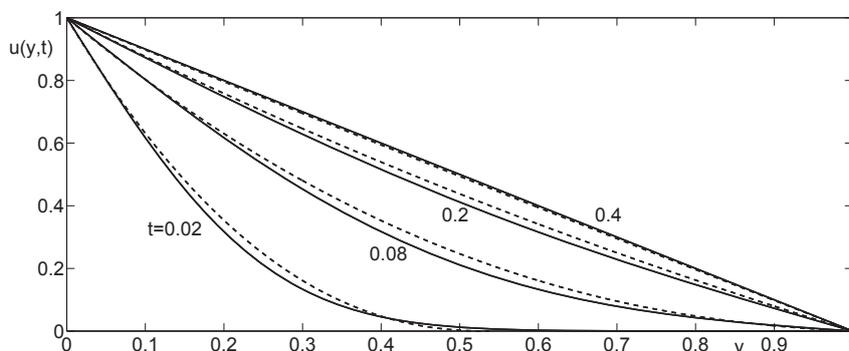

FIGURE 1. *Comparison of separable (solid) and HBIM (dashed) solutions at times $t = 0.02, 0.08, 0.2, 0.4$*

In the r, θ system we may write the temperatures as

$$(35) \qquad \theta_e = T_c + (1-T_c)r^{n-1}$$

$$(36) \qquad \theta_s = 1 + \sum_{n=1}^{N} 2\frac{(-1)^n}{\pi n r} \sin(n\pi r)e^{-n^2\pi^2\alpha' t},$$

where the first equation holds for $t > t'_1$. The temperature at the centre predicted by the HBIM is zero for $t \leq t'_1$ and $T_c(t)$ for $t \geq t'_1$. For the separable solution

the centre temperature is

$$(37) \qquad \theta_s(0,t) = \lim_{r \to 0} \frac{u_s(r,t)}{r} = 1 + \sum_{n=1}^{N} 2(-1)^n e^{-n^2 \pi^2 \alpha' t}.$$

Figure 2 shows a comparison of $T_c(t)$ and $\theta_s(0,t)$. The HBIM solution is the dotted line which begins at $t_1' = 0.069$ and steadily rises to the asymptote of $T_c = 1$ (the steady-state solution is that the temperature everywhere matches the boundary temperature $\theta(1,\infty) = 1$). The solid line is the separable solution, which shows that the centre temperature is indeed close to zero for some time, but it does start to increase noticeably earlier than the HBIM solution. For $t > 0.1$ the HBIM solution predicts a slightly higher temperature but in general the agreement is reasonable.
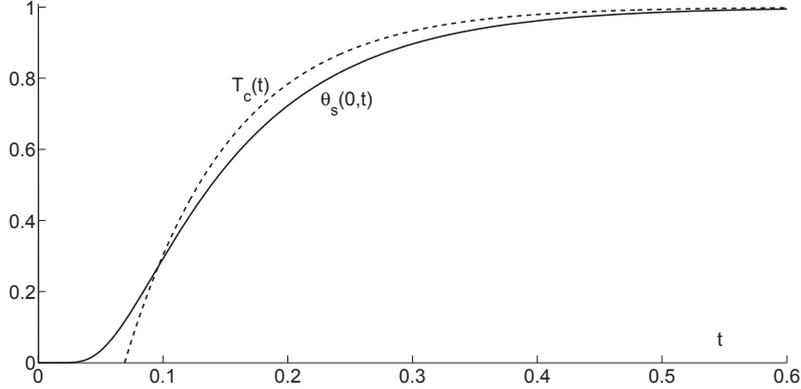

FIGURE 2. *Comparison of $T_c(t)$ and $\theta_s(0,t)$*

The goal of this exercise is to find an equivalent fluid that behaves in a similar manner to the fluid with a nanoparticle. Now the HBIM solution has been shown to be reasonably accurate we may achieve this goal by some form of matching of the HBIM solution with a particle and for the equivalent fluid. In this case we take the simple option of equating the decay rates in the expressions for T_p and T_c (since this forces the temperature profiles to be similar). This is equivalent to setting $\Lambda = \Lambda'$ and gives

$$(38) \qquad \alpha_e = \frac{\alpha_l}{(1-r_p)^2} \frac{n-1}{2(n+1)} \left[\frac{1+r_p}{2} - \frac{1}{n+1} \right]^{-1}.$$

The radius r_p is non-dimensional, scaled with the fluid radius R. We may express this result in a more standard form via equation (11), which states $r_p = \phi^{1/3}$,

$$(39) \qquad \alpha_e = \frac{\alpha_l}{(1-\phi^{1/3})^2} \frac{n-1}{2(n+1)} \left[\frac{1+\phi^{1/3}}{2} - \frac{1}{n+1} \right]^{-1}.$$

Hence the thermal diffusivity of the equivalent fluid depends only on the liquid diffusivity and volume fraction (the value of $n = 2.233$ is fixed). The composition of the nanoparticle does not affect α_e. Noting that $\alpha_e = k_e/(\rho c)_e$ and $(\rho c)_e = \phi \rho_p c_p + (1 - \phi) \rho_l c_l$, see (Zhou & Rui, 2008), we may write the effective thermal conductivity as

$$(40) \qquad k_e = \frac{k_l}{(1 - \phi^{1/3})^2} \left[(1 - \phi) + \phi \frac{\rho_p c_p}{\rho_l c_l} \right] \frac{n - 1}{2(n + 1)} \left[\frac{1 + \phi^{1/3}}{2} - \frac{1}{n + 1} \right]^{-1}$$

According to this formula, the equivalent fluid conductivity does depend on the particle properties, through $(\rho c)_p$, but there is no dependence on k_p. However, since the ratio $\rho_p c_p/(\rho_l c_l)$ is order 1 and ϕ is small this is a weak dependence.

In proposing the above formula for the effective diffusivity and conductivity we must stress the limitations of these results. The reduction of the governing equations was based on the observation that α_p/α_l, k_p/k_l are both large for the systems given in Table 1 but this may not be true for all nanofluid systems. So the errors associated with the approximations will increase as the α and k ratios decrease (for example with ceramic and organic particles). Philip and Shima (Philip & Shima, 2012) discuss a wealth of experiments and devote a section to the effect of nanoparticle material on the nanofluid properties. They quote studies, including their own, that indicate k_p is not an important factor in determining k_e (they also quote results leading to the opposite conclusion). The above formula indicates that the key particle parameter is $\rho_p c_p$. This does not appear to have been studied. In the cases where α_l/α_p, k_l/k_p are not negligible then our approximations do not hold and the nanoparticle properties will become important in determining α_e, k_e.

4. Comparison with experiment

The true test of a theory comes through comparison with experiment. In Figures 3, 4 we compare the present prediction for k_e with that of Maxwell and a number of data sets taken from the literature. The most common technique used to obtain data was the Transient Hot Wire technique. As mentioned in the introduction, there are many discrepancies between experimental data sets, see (Buongiorno et al., 2009; Eastman et al., 2004; Eastman et al., 2001; Koo & Kleinstreuer, 2004; Prasher et al., 2005), and so we cannot hope to match all points. Figure 3 shows results for an Al_2O_3-water nanofluid. The predicton of the current theory, given by equation (40), is shown as the solid line, the Maxwell result of equation (1) is the dashed line. For very low volume fractions the Maxwell curve lies above ours and captures the data better, but for $\phi > 0.008$ the present model rapidly increases above Maxwell and, more importantly, passes between a large amount of the experimental data. The slight dip in the solid line is an artefact of the approximation method, which loses accuracy as ϕ and hence $r_p \to 0$. In contrast to the Maxwell model, which becomes less accurate as ϕ
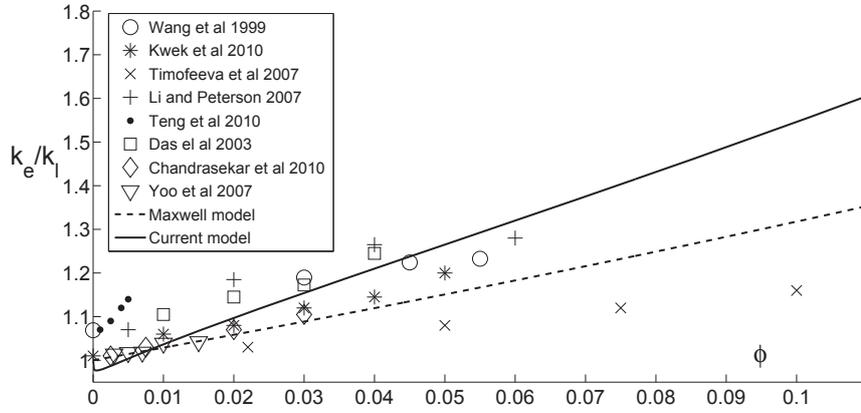
FIGURE 3. *Conductivity ratio k_e/k_l for Al_2O_3-water nanofluid with $k_l = 0.58\,W/mK$: equation* (40) *(solid line); Maxwell model equation* (1) *(dashed line); experimental data from (Wang* et al., *1999; Kwek* et al., *2010; Chandrasekar* et al., *2010; Teng* et al., *2010; Yoo* et al., *2007; Timofeeva* et al., *2007; Das* et al., *2003; Li & Peterson, 2007)*

increases our model becomes less accurate for very small ϕ. To be specific, to ensure that $k_e/k_l > 1$ our model requires volume fractions $\phi > 0.004$ or 0.4%.
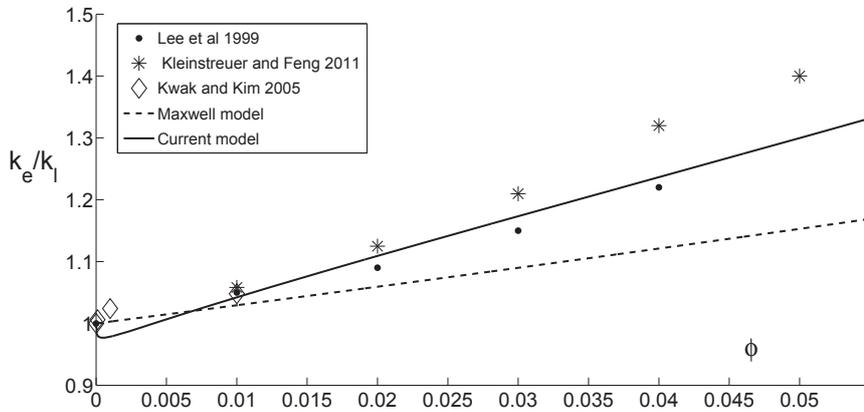

FIGURE 4. *Conductivity ratio k_e/k_l for CuO-ethylene glycol nanofluid with $k_l = 0.258\,W/mK$: equation* (40) *(solid line); Maxwell model equation* (1) *(dashed line); experimental data from (Kwak & Kim, 2005; Kleinstreuer & Feng, 2011; Lee* et al., *1999)*

Figure 4 shows results for a Cu-ethylene glycol nanofluid. In this case we only plot three sets of data points. Kwak and Kim (Kwak & Kim, 2005) only present one data point for $\phi > 0.005$, but this point lies close to our curve, the other two

data sets lie on either side of the present result. As the volume fraction increases the Maxwell model underpredicts the experimental data.

In both figures it is clear that the present model provides a much better approximation to the majority of experimental data when compared to the basic Maxwell model for volume fractions approximately greater than 1%.

5. CONCLUSION

The Maxwell model and its many variants are based on analysing steady-state heat flow over an infinite domain to provide an expression for the effective thermal conductivity of a nanofluid. The infinite domain assumption means the model is only valid for very disperse fluids. The theory developed in the present paper follows a different approach in that it analyses the dynamic behaviour of a nanofluid occupying a finite domain. Our analysis is based on a time-dependent model whereas the Maxwell model is steady-state. The majority of the experimental data was obtained using the Transient Hot Wire technique, that is, a time-dependent experiment. However, the conductivity should be a constant fluid property so although our approach may seem more suited to the experimental technique in fact it should be irrelevant whether data is obtained through transient or steady experiments.

Our model does not have the restriction of a disperse fluid, in fact it loses accuracy for very low volume fractions, below around 0.4%. Further, to make the analysis tractable we require the particle to have a much higher diffusivity and conductivity than the fluid (which is generally the case). This approach leads to a novel, simple analytical expression for the effective thermal conductivity. The model contains no unknown parameters, such as nanolayer properties. For volume fractions $\phi > 1\%$ it shows a greater enhancement than the Maxwell model and, most importantly, lies well within the values of k_e measured via numerous experiments up to high concentrations.

The variations that have been applied to the Maxwell model could also be applied to the present model. However, these modifications were motivated by the fact that Maxwell underpredicts the thermal conductivity. The present model, which predicts much higher conductivity suggests that perhaps these modifications are unnecessary. Put another way, the inability of the Maxwell model to capture the enhancement may be due to the limitations or unphysical assumptions of that model rather than any unusual nanoscale effect, such as the presence of nanolayers or aggregation.

There are many experiments indicating the dependence of k_e on quantities such as particle size, shape and material, additives, pH and temperature effects (Philip & Shima, 2012) (and many suggesting a lack of dependence (Philip & Shima, 2012)). Our analysis indicates the effective thermal diffusivity depends solely (to within an error of the order α_l/α_p) on ϕ and k_l, whilst the effective thermal conductivity depends primarily on these two parameters, with a small effect

coming from the product of particle density and specific heat, $\rho_p c_p$. However, these conclusions rely on the high conductivity and diffusivity ratios between the particle and base fluid which may not always be true. Organic or ceramic nanoparticles typically give lower values. When the difference between the particle and liquid thermal properties is not so large then other effects will enter into the expressions for conductivity and diffusivity. This could explain the dependence on other system properties mentioned above.

References

[1] J. Buongiorno, D.C. Venerus, N. Prabhat, T. McKrell, J. Townsend *et al.* A Benchmark study on the thermal conductivity of nanofluids. Journal of Applied Physics 106 (2009), 094312.

[2] M. Chandrasekar, S. Suresh and A.C. Bose. Experimental investigations and theoretical determination of thermal conductivity and viscosity of $Al_2O_3$3/water nanofluid, Experimental Thermal and Fluid Science 34:210-216, 2010.

[3] S.K. Das, S.U. Choi, W. Yu, T. Pradeep. Nanofluids: Science and Technology. John Wiley and Sons 2008.

[4] S.K. Das, N. Putra, P. Thiesen and W. Roetzel. Temperature dependence of thermal conductivity enhancement for nanofluids. Journal of Heat Transfer 125 (2003), 567–574.

[5] J.A. Eastman, S.R. Phillpot, S.U.S. Choi and P. Keblinski. Thermal transport in nanofluids. Annu. Rev. Mater. Res. 34:21946, 2004. doi: 10.1146/annurev.matsci.34.052803.090621

[6] J.A. Eastman, S.U.S. Choi, W. Yu and L.J. Thompson. Anomalously increased effective thermal conductivities of ethylene glycol-based nanofluids containing copper nanoparticles. Applied Physics Letters: volume 78, number 6, 2001.

[7] R.L. Hamilton and O.K. Crosser. Thermal conductivity of heterogeneous two component systems. Industrial and Engineering Chemistry Fundamentals 1. 1962.

[8] P. Keblinski, J.A. Eastman and D.G. Cahill. Nanofluids for thermal transport. Mater. Today 8 (2005), 36.

[9] P. Keblinski, S.R. Phillpot, S.U.S. Choi and J.A. Eastman. Mechanisms of heat flow in suspensions of nano-sized particles (nanofluids). Int. J. Heat Mass Trans. 45:855863, 2002.

[10] P. Keblinski, R. Prasher and J. Eapen. Thermal conductance of nanofluids: is the controversy over? Journal of Nanoparticle Research 10:1089–1097, 2008.

[11] C. Kleinstreuer and Y. Feng. Experimental and theoretical studies of nanofluid thermal conductivity enhancement: a review. Nanoscale Research Letters 6:229, 2011.

[12] J. Koo and C. Kleinstreuer. A new thermal conductivity model for nanofluids. Journal of Nanoparticle Research 6:577588, 2004.

[13] K. Kwak and C. Kim. Viscosity and thermal conductivity of copper oxide nanofluid dispersed in ethylene glycol. Korea-Australia Rheology Journal, vol. 17, no. 2, pp. 35–40, June 2005.

[14] D. Kwek, A. Crivoi and Fei Duan. Effects of temperature and particle size on the thermal property measurements of Al_2O_3-water nanofluids. J. Chem. Eng. Data 55 (2010), 5690–5695.

[15] S. Lee, S.U.S. Choi, S. Li and J.A. Eastman. Measuring thermal conductivity of fluids containing oxide nanoparticles. J. Heat Transfer 121 (1999), 280–289.

[16] C.H. Li and G.P. Peterson. The effect of particle size on the effective thermal conductivity of Al_2O_3-water nanofluids. Journal of Applied Physics 101 (2007).

[17] J.C. Maxwell. A treatise on electricity and magnetism, third edition, Clarendon Press, Oxford, UK, 1891.

[18] S.L. Mitchell and T.G. Myers. Application of standard and refined heat balance integral methods to one-dimensional Stefan problems. SIAM Review, 52 (2010), no. 1, 57–86.

[19] S.L. Mitchell and T.G. Myers. Improving the accuracy of heat balance integral methods applied to thermal problems with time dependent boundary conditions. International Journal of Heat and Mass Transfer volume: 53 Issue: 17-18 Pages: 3540–3551, 2010. doi: 10.1016/j.ijheatmasstransfer.2010.04.015

[20] S.L. Mitchell and T.G. Myers. Heat balance integral method for one-dimensional. finite ablation. Journal of Thermophysics and Heat Transfer, vol. 22, no. 3, July-September 2008.

[21] T.G. Myers. Optimizing the exponent in the heat balance and refined integral methods. Int. Comm. Heat Mass Trans. 36 (2009), no. 2, 143–147. doi: 10.1016/j.icheatmasstransfer. 2008.10.013.

[22] T.G. Myers. Optimal exponent heat balance and refined integral methods applied to Stefan problems. Int. J. Heat Mass Trans. 2010. doi: 10.1016/j.ijheatmasstransfer.2009.10.045

[23] J. Philip and P.D. Shima. Thermal properties of nanofluids. Advances in Colliod and Interface Science, volume 183:30–45, 2012.

[24] R. Prasher, P. Bhattacharya and P.E. Phelan. Thermal conductivity of nanoscale colloidal solutions (nanofluids). Phys. Rev. Lett. 94 (2005), 025901.

[25] T.P. Teng, Y.H. Hung, T.C. Teng, H.E. Moa and H.G. Hsu. The effect of alumina/water nanofluid particle size on thermal conductivity, Applied Thermal Engineering 30:2213–2218, 2010.

[26] P. Tillman and J.M. Hill. Determination of nanolayer thickness for a nanofluid. International Communications in Heat and Mass Transfer 34:399–407, 2007.

[27] E.V. Timofeeva, A.N. Gavrilov, J.M. McCloskey, Y.V. Tolmachev, S. Sprunt, L.M. Lopatina and J.V. Selinger. Thermal conductivity and particle agglomeration in alumina nanofluids: experiment and theory. Physical Review E 76 (2007).

[28] X. Wang, X. Xu and S.U.S. Choi. Thermal conductivity of nanoparticle-fluid mixture, Journal of Thermophysics and Heat Transfer. vol. 13, no. 4, October-December 1999.

[29] B.X. Wang, L.P. Zhou and X.F. Peng. A fractal model for predicting the effective thermal conductivity of liquid with suspension of nanoparticles. Int. J. Heat & Mass Transf. 46:2665–2675, 2003.

[30] D.M. Wood and N.W. Ashcroft. Effective medium theory of optical properties of small particle composites. Philos. Mag. 35 (1977), no. 2, 269–280.

[31] D.H. Yoo, K.S. Hong, T.E. Hong, J.A. Eastman and H.S. Yang. Thermal conductivity of $Al_2O_3$3/water nanofluids. Journal of the Korean Physical Society, vol. 51, October 2007.

[32] W. Yu and S.U.S. Choi. The role of interfacial layers in the enhanced thermal conductivity of nanofluids: A renovated Maxwell model. Journal of Nanoparticle Research 5:167-171, 2003.

[33] W. Yu and S.U.S. Choi. The role of interfacial layers in the enhanced thermal conductivity of nanofluids: A renovated Hamilton-Crosser model. Journal of Nanoparticle Research 6:355-361, 2004.

[34] S.Q. Zhou and N. Rui. Measurement of the Specific Heat Capacity of Water-based Al_2O_3 Nanofluid. Applied Physics Letters 92 (2008), 093123.

T.G. Myers
Centre de Recerca Matemàtica
Campus de Bellaterra, Edifici C
08193 Bellaterra, Barcelona, Spain
Tel.: +34-935868517
Fax: +34-935812202
   E-mail address: tmyers@crm.cat

M.M. MacDevette
Centre de Recerca Matemàtica
Campus de Bellaterra, Edifici C
08193 Bellaterra
Barcelona, Spain
and
Departament de Matemàtica Aplicada I
Universitat Politècnica de Catalunya
Barcelona, Spain
   E-mail address: mmacdevette@crm.cat

H. Ribera
Centre de Recerca Matemàtica
Campus de Bellaterra, Edifici C
08193 Bellaterra
Barcelona, Spain